# Adsorption and switching behavior of individual Ti atoms on the Si(111)-7×7 surface

H. F. Hsu,[1] L. J. Chen,[1] H. L. Hsiao,[2] and T. W. Pi[3]
[1]*Department of Materials Science and Engineering, National Tsing Hua University, Hsinchu, Taiwan, Republic of China*
[2]*Department of Physics, Tunghai University, Taichung, Taiwan, Republic of China*
[3]*Synchrotron Radiation Research Center, Hsinchu, Taiwan, Republic of China*
(Received 24 February 2003; revised manuscript received 28 May 2003; published 7 October 2003)

The adsorption and switching behaviors of Ti atoms on Si(111)-7×7 surfaces for room-temperature and 100 °C depositions have been investigated by successive scanning tunneling microscope (STM) imagings of the same region as well as by synchrotron radiation ultraviolet photoemission spectroscopy (SR-UPS). At very low coverage (0.02 monolayer), individual Ti atoms are confined and switched within the ''subtriangular'' region consisting of two neighboring center adatoms and corresponding corner adatom in a half unit cell at room temperature. Both STM and SR-UPS data indicate that the individual Ti atoms adsorbed are associated with the Si rest atom sites. The Ti atoms were found to be more mobile in faulted halves than that in unfaulted halves.

DOI: 10.1103/PhysRevB.68.165403 PACS number(s): 68.37.Ef, 68.35.Ja, 68.35.Md

## I. INTRODUCTION

The surface diffusion of adsorption atoms is an important subject of surface science and the scanning tunneling microscope (STM) is a powerful tool for observation of the diffusion of individual atoms on semiconductor surfaces.[1–6] Ti/Si is a technologically important system. For the initial growth at room temperature, Ti-Si reactivity has been known to be very strong.[7–11] The adsorption and reaction of Ti on Si(111)-7×7 surfaces have been studied using STM.[12,13] The main effort has been directed to the analysis of high-coverage and high-temperature reactions, somehow bypassing the very early stages of Ti-Si reactions at room temperature. In this paper, the results of a STM and synchrotron radiation ultraviolet photoemission spectroscopy (SR-UPS) investigation of the adsorption and switching of individual Ti atoms at room temperature on Si(111)-7×7 surfaces are presented. Ultralow-coverage deposition and observations of very long periods of time have enabled us to analyze the trapping characteristics of mobile Ti adatoms in the reconstructed cells. Exceptionally sharp surface emission obtained by SR-UPS provides pertinent information on the surface reaction.

## II. EXPERIMENTAL PROCEDURES

The STM experiments were carried out in an ultrahigh-vacuum (UHV) chamber with a base pressure below $5\times10^{-11}$ mbar. The chamber is equipped with an ultrahigh-vacuum STM (Omicron STM1). All STM images were taken at room temperature in the constant-current mode with a tunneling current of ~0.2 nA. Si(111) substrates with miscut orientation of less than 0.5° (P doped, 0.1–0.2 Ω cm, 10 mm×4 mm×0.3 mm) were used. After introducing the samples into the chamber, 7×7 reconstruction was achieved by direct current heating at ~700 °C for several hours followed by flashing several times at 1250 °C for a total of 1 min below $1\times10^{-9}$ mbar. Samples were checked to ensure that they had a well-ordered 7×7 surface before any metal deposition. The evaporation of Ti (99.99% purity) was performed with a well-outgassed electron-beam evaporator at room temperature or 100 °C. During the evaporation the pressure in the chamber was better than $1\times10^{-10}$ mbar. The deposition rate was about 0.16 ML/min, where one monolayer (ML) is defined to consist of $7.83\times10^{14}$ atoms/cm$^2$, corresponding to one adsorption atom per ideal Si(111)-1×1 surface atom. The valence-band spectra were taken in the low-energy spherical grating monochromator beamline (LSGM, BL-08A) at Synchrotron Radiation Research Center (SRRC) in Hsinchu, Taiwan.

## III. RESULTS

Figure 1 presents an occupied-state STM image of Ti/Si(111)-7×7 at 0.007 ML. At this ultralow coverage, the surface retains the original 7×7 reconstruction. Some adatoms including center and corner adatom sites in both faulted or unfaulted half unit cells appear brighter. These brighter adatom are mobile as shown in Fig. 2.

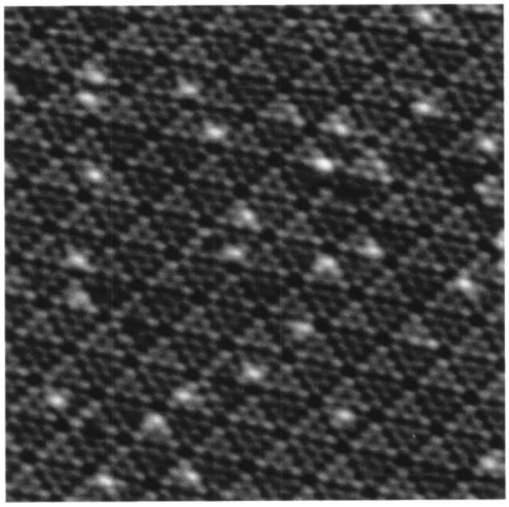

FIG. 1. Filled-state STM image ($V_s=-2$ V) showing the Si(111)-7×7 surface with ~0.007 ML of Ti.

 

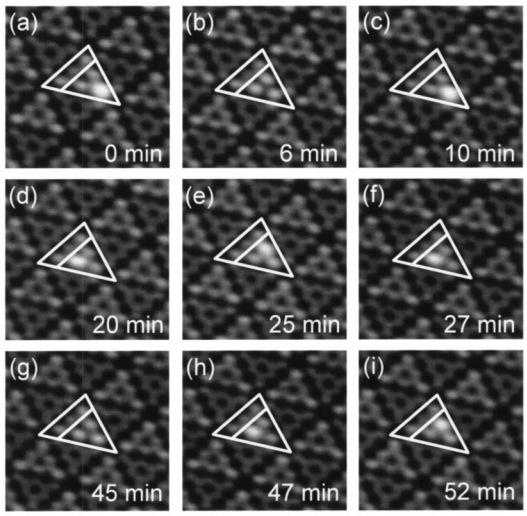


FIG. 2. Consecutive STM micrographs showing the hopping of a Ti atom at room temperature. (a), (c) are at the *C* site, (b), (g) are at the *A* site, and (d)–(f), (h), and (i) are at the *B* site.

Figure 2 shows nine filled-state images that are selected from a sequence of successive STM images, obtained at room temperature, of the same region. In the outlined faulted half, a subtriangle (also outlined) consisting of two center adatoms and corresponding corner adatom is of particular interest. In these images, either one of the three adatoms [Figs. 2(a), 2(c)–2(f), and 2(h) and 2(i)] or all three adatoms [Figs. 2(b) and 2(g)] becomes brighter. In addition, no matter how the bright site changes, the bright adatom is always confined in this subtriangular region. As will be shown in later paragraphs, the Ti atom is actually not adsorbed right on the top of the Si adatoms to make the adatoms appear brighter.

Figure 3 shows the dimer-adatom-stacking (DAS) fault model of the faulted half of the Si(111)-7×7 reconstruction. Figure 3(a) corresponds to the STM image of the faulted subunit cell enclosed in the bright triangle in Fig. 2(a). Figure 3(b) is a cross-sectional view along the long diagonal showing the vertical extension of the Si atoms of a 7×7 unit cell. If a Ti atom were adsorbed on top of the center adatom so that the center adatom appears brighter, the bright site should have the same probability to hop between three center adatoms (labeled *h*, *k*, and *l* in Fig. 3). But from the consecutive STM images obtained with a time interval of about 100 s for 2 h, the hopping of the brighter adatom from *h*, *k*, to the *l* center adatom site was never observed. As a result, the Ti atoms are confined in the subtriangular region consisting of two center adatoms and the corresponding corner adatom (labeled *h*, *k*, and *c* in Fig. 3). It indicates that once a Ti atom is trapped within the subtriangular region, it can never escape at room temperature.

The types of adsorption sites were defined visually by STM images with different sample bias voltages (from −2 V to 2 V) and quantitatively by line scans in the images with −2 V sample bias. We note that, in addition to the three most common types of adsorption sites—i.e., sites *A*, *B*, and *C* (shown as follows)—a small fraction (about 5%) of images

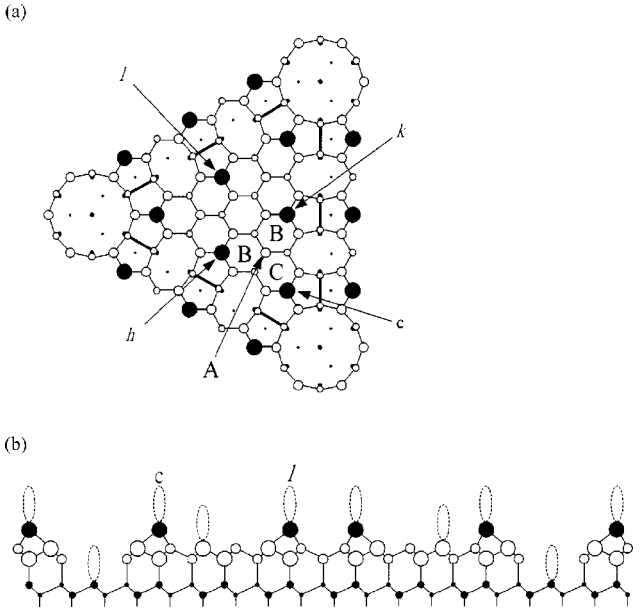


FIG. 3. The atomic model of the faulted half of the Si(111)-7×7 reconstruction corresponding to the faulted subunit cell in Fig. 1(a) enclosed in the bright triangle. Site *A* is on top of the rest atom. Site *B* is between the rest atom and center adatom. Site *C* is between the rest atom and corner adatom. *h*, *k*, and *l* indicate three center adatoms in this faulted subunit cell. *c* indicates the corresponding corner adatom of *h* and *k* center adatoms.

that are of different types is yet to be interpreted and not reported herein.

For a Ti atom trapped at site *A*, as seen in Figs. 2(b) and 2(g), three adatoms become brighter simultaneously in the filled-state images and the apparent height of the brighter adatoms is higher than usual by about 0.5 Å with −2 V bias as shown in Figs. 4(a) and 4(b). The empty-state images are identical to those of the clean Si(111)-7×7 surface. From a consideration of the image symmetry, the most probable site for a Ti atom is on top of the rest atom, similar to Au-atom adsorption on top of the rest atom of the Si(111)-7×7 surface.[14] The reaction of the rest atoms would cause a reverse charge transfer from the reacted rest atoms to surrounding atoms and thus make those adatoms appear brighter.[6]

For site-*B* adsorption, as seen in Figs. 2(d)–2(f), 2(h), and 2(i), there is one brighter center adatom and the apparent height of it is higher than usual by about 1.2 Å with −2 V bias as shown in Figs. 4(a) and 4(c).

In the empty-state image, the bright spot was found to be not right at the center adatom site. Figure 5 displays two image brightness profiles along the $[\bar{1}\bar{1}2]$ direction with 1 V sample bias. A clean unit cell is traced in profile *XY* and two dotted lines indicate the positions of the center adatom and the rest atom. The profile $X'Y'$ passes through a subunit cell containing site-*B* adsorption of a Ti atom. The peak associated with the site-*B* adsorption is located between a rest atom and a neighboring center adatom, as marked by the open arrow in Fig. 5.

A previous analysis of single Si atoms deposited on the Si(111)-7×7 surface concluded that the center of a bright

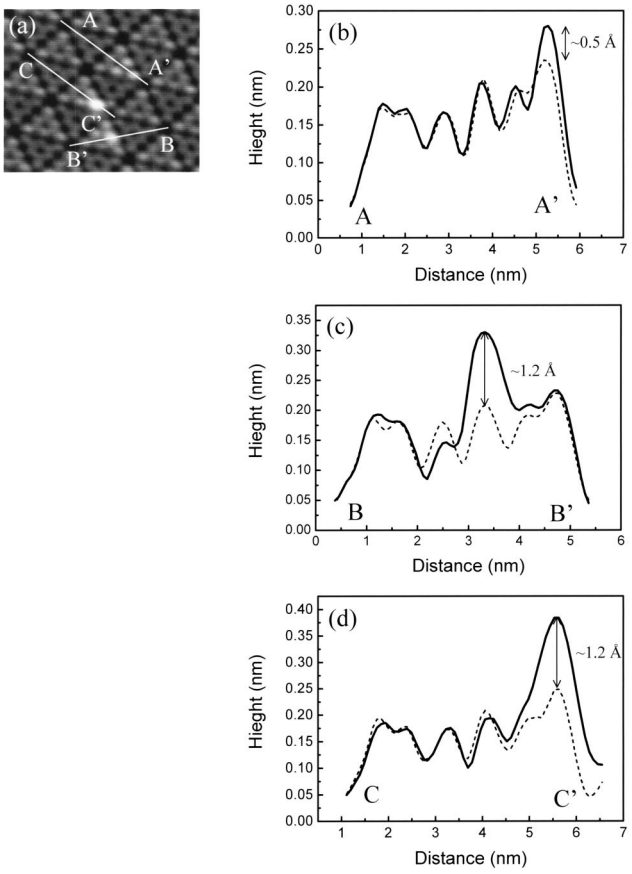


FIG. 4. (a) Filled-state image, $V_s=-2$ V, of site-*A*, -*B*, and -*C* adsorption. Image brightness profiles along the $AA'$, $BB'$, and $CC'$ lines are shown in (b), (c), and (d), respectively. The dashed lines are for the clean unit cells.

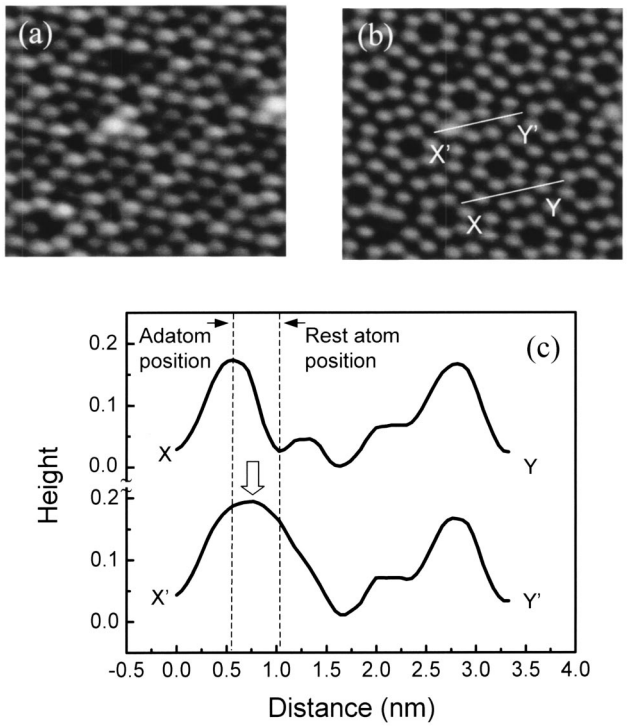


FIG. 5. (a) Filled-state image, $V_s=-1$ V and (b) empty-state image, $V_s=1$ V of site-*B* adsorption. (c) Image brightness profiles along the $XY$ and $X'Y'$ lines indicated in (b). Profile $XY$ is for a clean unit cell while profile $X'Y'$ is for a site-*B* adsorption in a faulted half and one in a clean unfaulted half.

extra spot in an empty-state STM image corresponds to the position of a deposited atom.[15] On the other hand, in the filled-state image, the redistribution of electron density is such that the center adatom looks brighter. It is worthwhile to note that the center of the maximum does not necessarily represent the position of an atom. The adsorption site is inferred not only from a comparison of the empty-state image and filled-state image, as shown in Fig. 5, but also from the hopping behavior of the brighter site on top of the Si adatom in the filled-state image. Otherwise, the bright site may jump out of the subtriangle from symmetry considerations. The analysis indicates that the Ti atom is adsorbed between a rest atom and a neighboring center adatom for site-*B* adsorption.

For site-*C* adsorption, as seen in Figs. 2(a) and 2(c), one corner adatom becomes brighter and the apparent height of the brighter corner adatom is higher than usual by about 1.2 Å with $-2$ V bias as shown in Figs. 4(a) and 4(d). The corner adatom is of too high a brightness to obscure the change in the line profiles near the rest adatom. On the other hand, from the analysis of the brightness profiles, shown in Figs. 6(b) and 6(c), at $-1$ V bias voltage, a significant change near the rest atom is apparent. It is therefore inferred that the Ti atom is adsorbed between the rest atom and corner adatom.

The UPS data also supported the identification of *A*, *B*, and *C* adsorption sites to be associated with the rest atom. Figure 7 shows the normalized valence-band spectra with exceptionally sharp surface-state emission. In the figure, $S_1$, $S_2$, and $S_3$, located at 0.3, 0.9, and 1.8 eV binding energy, are known to correspond to the adatom (AD), rest atom (R), and adatom-backbond (ADB) surface states, respectively.[17,18] As seen in the figure, deposition of Ti quenches first the surface states $S_1$ and $S_2$, which become fully attenuated at about 0.24 ML, while $S_3$ appears to be less influenced. With 0.02 ML Ti coverage, the intensity of the $S_2$ state decreases while that of the $S_1$ state stays the same. This indicates that at this coverage Ti interacts first with the rest atom. Comparing with the STM images and the line scans of 0.007 ML coverage with various sample biases as shown in Fig. 8 as well as Figs. 9, 10, and 11, the adsorption types of 0.02 ML deposition were found to be the same as those of 0.007 ML deposition.

The relative brightness and height of the brighter adatom are lower at $-1$ V sample bias than at $-2$ V sample bias. At $-0.5$ V sample bias, the relative brightness and height of the adatom are even lower and not readily detected. From the results of UPS measurements, shown in the Fig. 7, the intensity of the $S_2$ state decreases while that of the $S_1$ state stays the same and that of the $S_3$ state increases slightly. As is well known, STM is not only sensitive to the surface geometry but also to the surface electronic structure. The measured tunneling current was proportional the integration of the density of surface states (DOS) from the Fermi energy to the

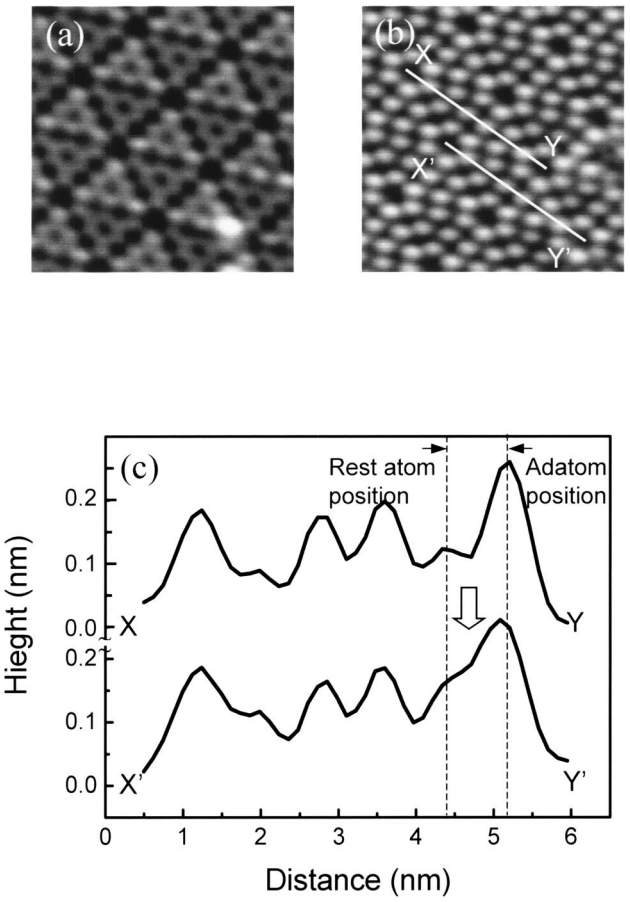


FIG. 6. (a) Filled-state image, $V_s=-2$ V and (b) empty-state image, $V_s=-1$ V of site-$C$ adsorption. (c) Image brightness profiles along the $XY$ and $X'Y'$ lines indicated in (b). Profile $XY$ is for a clean unit cell while profile $X'Y'$ is for a site-$C$ adsorption in a faulted half extended from a clean unfaulted half.

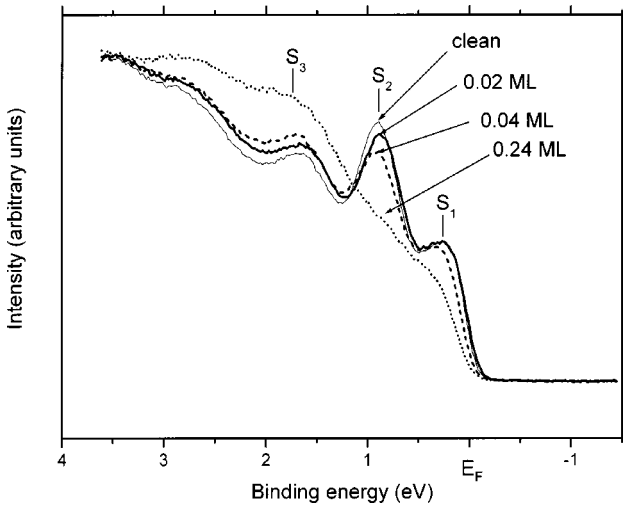


FIG. 7. The valence-band spectra of $\leqslant 0.24$ ML depositions after normalization. The characteristic surface states $S_1$, $S_2$, and $S_3$ corresponding to the adatom dangling bonds, rest-atom dangling bonds, and the adatom back bonds, respectively.

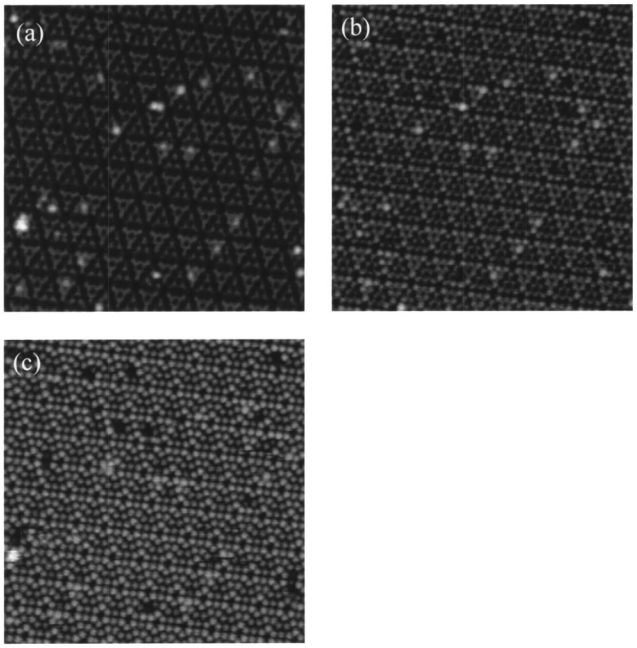


FIG. 8. Filled-state STM image showing the Si(111)-7×7 surface deposited with ~0.007 ML Ti with (a) $V_s=-2$ V, (b) $V_s=-1$ V, and (c) $V_s=-0.5$ V.

bias voltage. With a sample bias voltage of $-0.5$ V, the DOS of $S_1$ was measured primarily. From a slightly more obvious variation of the brightness of the adatom with a sample bias voltage $-0.5$ V than that of $-2$ V and $-1$ V and on a change of $S_1$ state in UPS analysis for Ti adsorbing, it was inferred that the Ti atoms were not adsorbed on the adatoms. Furthermore, the increase of the adatom brightness is due to the charge redistribution by the interaction of Ti atoms with the rest atoms. The adatoms becomes brighter at $-2$ V sample bias since the DOS of $S_3$ increases.

For faulted halves, the relative hopping probabilities of $A_f \rightarrow B_f$, $B_f \rightarrow A_f$, and $B_f \rightarrow B_f$ are 38%, 38%, and 15%, respectively, where the subscript "f" refers to the faulted half unit cell. The probability of all hopping to and from the $C$ configuration ($A_f \rightarrow C_f$, $B_f \rightarrow C_f$, $C_f \rightarrow A_f$, and $C_f \rightarrow B_f$) is about 9%. The Ti atoms in the unfaulted "u" half unit cells are of nearly zero mobility. Only a few hopping incidents ($B_u \rightarrow B_u$) in the unfaulted halves were observed in our continuous-time imaging for 2 h. The observation indicates that the mobility of single Ti atoms in the faulted halves is much higher than that in the unfaulted halves, especially between two adjacent $B$ sites and between $A$ and $B$ sites.

Limited by the scanning speed of the STM used (about 100 s for a $30\times30$ nm$^2$ frame), caution needs be exercised in the possible overlook of some of the hopping events from the consecutive STM images. In addition, whether the distribution of Ti atoms has reached equilibrium is of critical concern. Consequently, as many as 700 adsorption sites for samples with Ti deposited at room temperature and 100 °C were analyzed to obtain a statistically more meaningful distribution as shown in Fig. 12. The population densities of Ti atoms on the faulted halves and unfaulted halves are statistically equal for room-temperature deposition. However, a

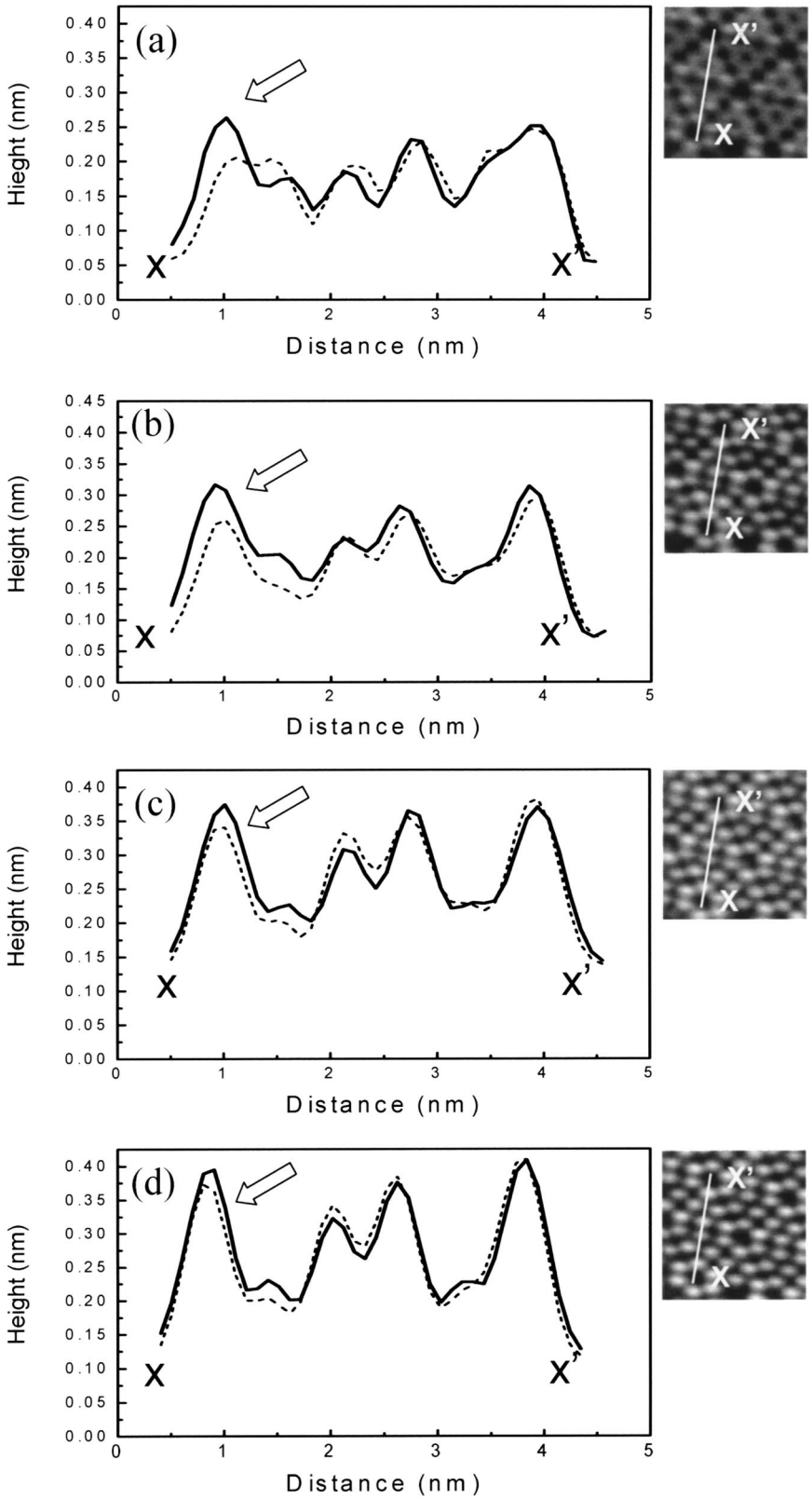


FIG. 9. The line scans of the site-*A* adsorption using various bias: (a) $V_s=-2$ V, (b) $V_s=-1.5$ V, (c) $V_s=-1$ V, and (d) $V_s=-0.5$ V with their corresponding STM images. The open arrows point to the brighter corner adatom due to Ti adsorbed at site *A*.

preference for faulted halves was observed for 100 °C depositions. It is apparent that, at room temperature, there is not enough energy for Ti to jump across the dimer to neighboring half unit cells. On the other hand, at 100 °C, Ti atoms can jump out of the half-triangles and reside preferentially on the faulted side. In the faulted subunits, the adsorption probabilities of sites *A*, *B*, and *C* are nearly equal. The proportion of type-*C* adsorption reduced significantly to almost nil

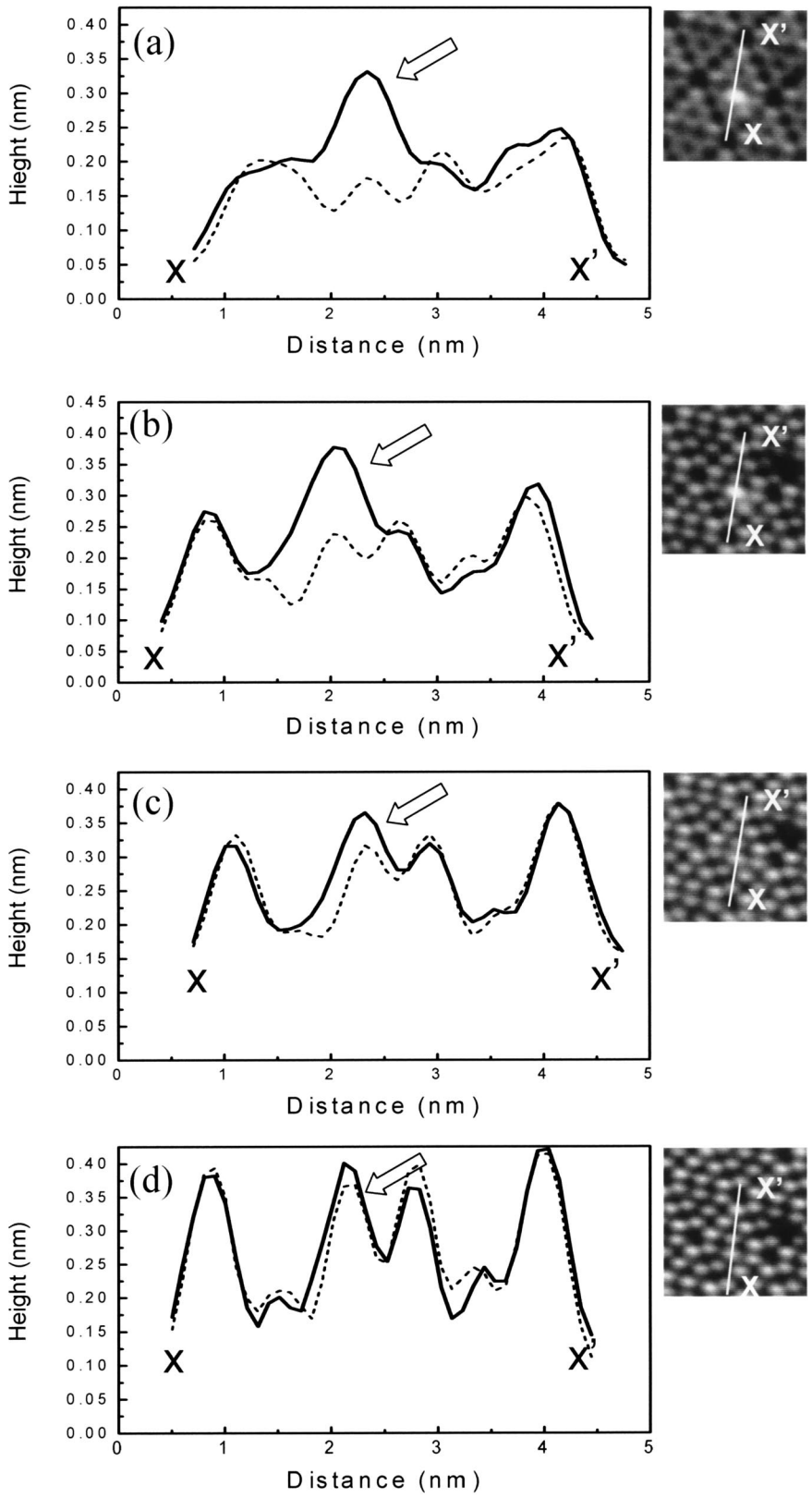


FIG. 10. The line scans of the site-*B* adsorption using various bias: (a) $V_s=-2$ V, (b) $V_s=-1.5$ V, (c) $V_s=-1$ V, and (d) $V_s=-0.5$ V with their corresponding STM images. The open arrows point to the brighter center adatom due to Ti adsorbed at site *B*.

in 100 °C deposited samples.

As seen in Figs. 3(a) and 3(b), the structural environments for sites *B* and *C* are significantly different. It is apparent that site *C* corresponds to an energy valley with steep slope and the energy barriers for Ti atom to jump in and out of site *C* to sites *A* or *B* are relatively high and difficult to overcome at room temperature. On the other hand, the adsorption probabilities at different sites are markedly different between

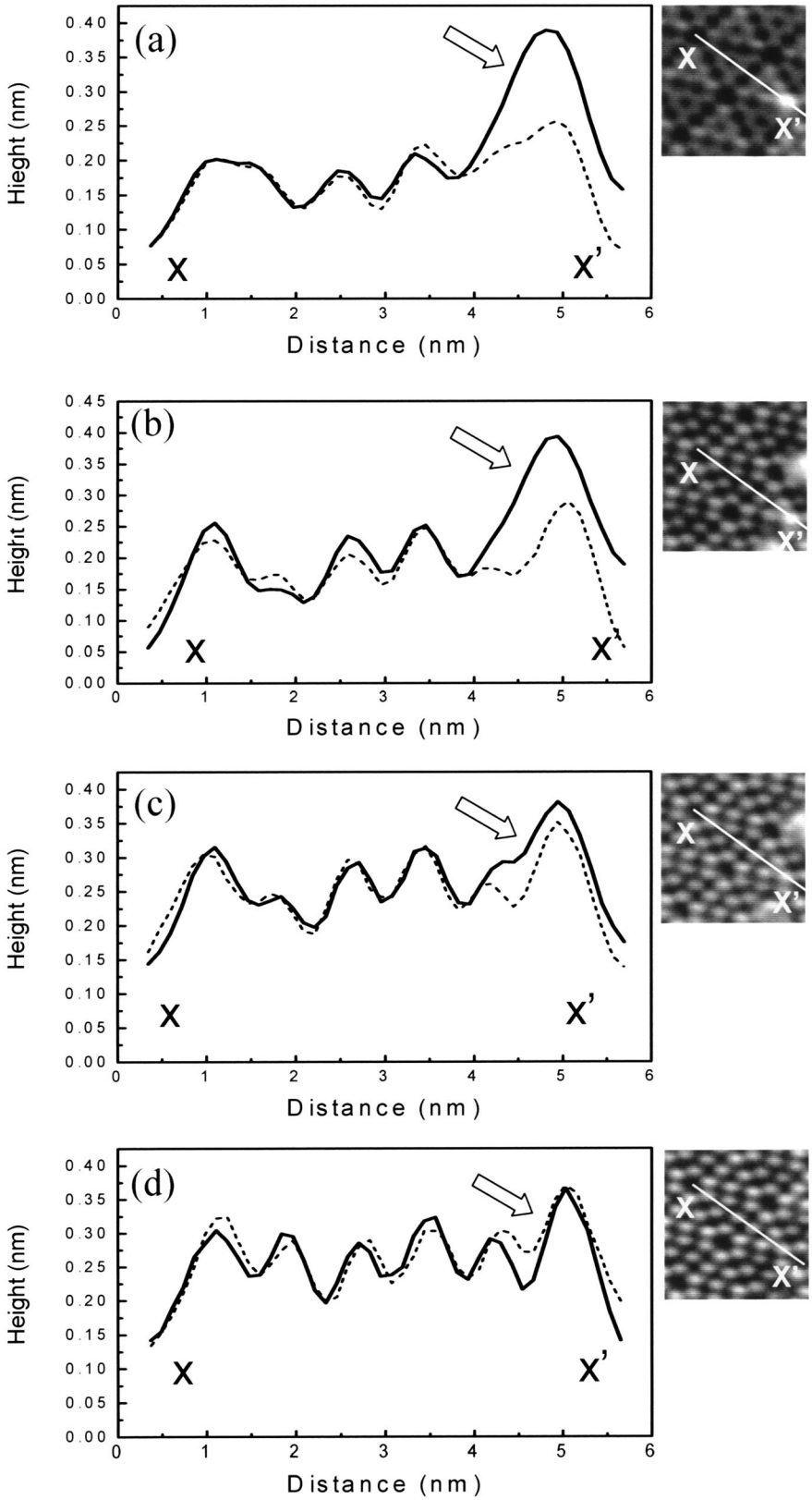


FIG. 11. The line scans of the site-*C* adsorption using various bias: (a) $V_s=-2$ V, (b) $V_s=-1.5$ V, (c) $V_s=-1$ V, and (d) $V_s=-0.5$ V with their corresponding STM images. The open arrows point to the brighter corner adatoma due to Ti adsorbed at site *C*.

faulted and unfaulted halves in both room-temperature and 100 °C deposited samples. In 100 °C deposited samples, Ti atoms, aided by the thermal energy, can jump more easily from site *C* to the site *A* or *B*. However, the reverse jump is more difficult owing to the higher energy barriers. In the unfaulted subunit, the binding energy for site *B* is obviously higher than those of the other sites since only the proportion of site-*B* adsorption increased and sites *A* and *C* are decreased in samples deposited at 100 °C. From the change of the adsorption site distributions between room-temperature

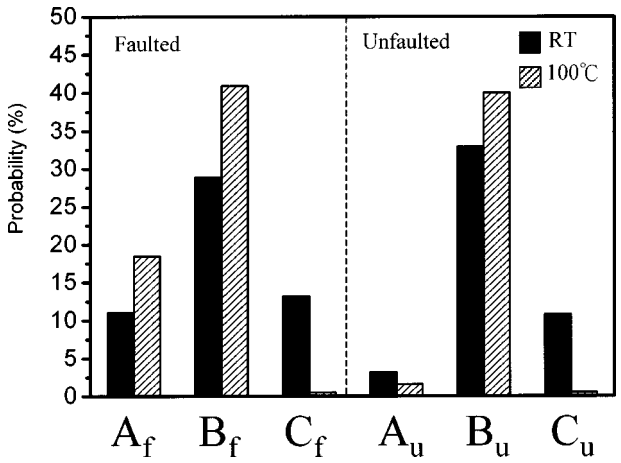


FIG. 12. Site populations for deposition temperature of room temperature and 100 °C. *A*, *B*, and *C* represent three kinds of the adsorption types. The subscript "f" represents Ti atom in the faulted half unit cell and "u" represents in the unfaulted unit cell.

and 100 °C deposition and fewer hopping incidents to and from site *C* in the faulted halves, it is inferred that the energy barrier between sites *C* and *B* or *C* and *A* is higher than that between two adjacent sites *B* or sites *A* and *B* at room temperature. The Ti atoms in the unfaulted halves are of nearly zero mobility. Consequently, no meaningful statistics can be obtained for hopping frequency.

## IV. DISCUSSION

From *ab initio* density functional theory calculations, it was concluded that the dangling bonds on the surface provide natural adsorption sites for adsorbed species.[19] The conclusion is consistent with the experimental findings of many gas/Si(111)-7×7 systems.[5,19] However, for transition-metal/Si(111)-7×7 systems, the relatively low coordination of Si dangling bonds adsorption sites makes them an implausible location for transition metals, which bond with six or more neighbors in bulk silicide compounds. The metal atoms were found to adsorb not just on top of the adatoms or rest atoms. For example, Co is adsorbed at the interstitial sites.[20] From our experiments, the preferential adsorption site is between the rest atom and neighboring center adatom (site *B*). The result is similar to the Ti/Si(100)-2×1 system,[7] in which a Ti atom is adsorbed at the pedestal site on the dimer row below 440 K and stronger chemical reactions occurred by substituting the Si dimer at higher temperatures.

The higher mobility of adsorption atoms in faulted half unit cells implies that there are several stable adsorption sites and the energy barriers between them are smaller than those in unfaulted halves. At room temperature, the individual Ti atom, once trapped, can never escape from the subtriangular region. The behaviors of Ti adsorbates on the Si(111)-7×7 surface at higher temperature as well as at higher coverage are currently under investigation and will be reported elsewhere.[16]

An alternative description of many of the effects observed might be that the Ti atom rests on the rest atom (*A*) and may tilt in various ways to interact with either the corner or edge adatoms. However, for 100 °C deposited samples, the adsorption at *C* sites becomes almost nil. This makes the alternative interpretation less likely since once the Ti atom is adsorbed on top of the rest atom, tilting toward *C* site should also occur.

## V. CONCLUSIONS

In conclusion, the adsorption and switching of single Ti atoms on Si(111)-7×7 surface have been investigated by STM and SR-UPS. Ti atoms are confined within a "subtriangular" region defined by two neighboring center adatoms and their corresponding corner adatom in the faulted halves of the 7×7 triangle at room temperature. Both STM and SR-UPS data indicate that the individual Ti atoms adsorbed are associated with the Si rest atom sites. Ti atoms were found to be more mobile in faulted halves than that in unfaulted halves at room temperature.

## ACKNOWLEDGMENTS

This research was supported by the Republic of China National Science Council Grant No. NSC 91-2215-E-007-002 and Ministry of Education Grant No. 91-E-FA04-1-4.

[1] I. S. Hwang and J. Golovchenko, Science **258**, 1119 (1992).
[2] H. Hibino and T. Ogino, Phys. Rev. B **55**, 7018 (1997).
[3] J. M. Gómez-Rodríguez, J. J. Sáenz, A. M. Baró, J. Y. Veuillen, and R. C. Cinti, Phys. Rev. Lett. **76**, 799 (1996).
[4] Y. W. Mo, Phys. Rev. Lett. **71**, 2923 (1993).
[5] R. L. Lo, I. S. Hwang, M. S. Ho, and T. T. Tsong, Phys. Rev. Lett. **80**, 5584 (1998).
[6] R. L. Lo, M. S. Ho, I. S. Hwang, and T. T. Tsong, Phys. Rev. B **58**, 9867 (1998).
[7] K. Ishiyama, Y. Taga, and A. Ichimiya, Phys. Rev. B **51**, 2380 (1995).
[8] M. delGiudice, J. J. Joyce, M. W. Ruckman, and J. H. Weaver, Phys. Rev. B **35**, 6213 (1987).
[9] X. Wallart, J. P. Nys, H. S. Zeng, G. Dalmai, I. Lefebvre, and M. Lannoo, Phys. Rev. B **41**, 3087 (1990).
[10] M. H. Wang and L. J. Chen, Appl. Phys. Lett. **59**, 2460 (1991).
[11] L. J. Chen, Mater. Sci. Eng., R. **29**, 115 (2000).
[12] S. Shingubara, S. Takata, E. T. Kahashi, S. Konagata, H. Sakaue, and T. Takahagi, in *Silicide Thin Films—Fabrications, Properties and Applications*, edited by R. T. Tung, K. Maex, P. W. Pellegrini, and L. H. Allen, Mater. Res. Soc. Symp. Proc. No. 402 (Materials Research Society, Pittsburgh, 1996), p. 137.
[13] K. Ezoe, H. Kuriyama, T. Yamamoto, S. Ohara, and S. Matsumoto, Appl. Surf. Sci. **130–132**, 133 (1998).
[14] I. Chizhov, G. Lee, and R. F. Willis, Phys. Rev. B **56**, 12 316 (1997).
[15] H. Uchida, S. Watanabe, M. Mase, H. Kuramochi, and M. Aono, Thin Solid Films **369**, 73 (2000).

[16] H. F. Hsu, M. C. Lu, C. K. Fang, H. L. Hsiao, and L. J. Chen (unpublished).
[17] R. Losio, K. N. Altmann, and F. J. Himpsel, Phys. Rev. B **61**, 10 845 (2000).
[18] A. L. Wachs, T. Miller, A. P. Shapiro, and T. C. Chiang, Phys. Rev. B **35**, 5514 (1987).
[19] K. D. Beommer, M. Galván, A. D. Pino, Jr., and J. D. Joannopoulos, Surf. Sci. **314**, 57 (1994).
[20] P. A. Bennett, D. G. Cahill, and M. Copel, Phys. Rev. Lett. **73**, 452 (1994).